

N74-10351

CASE FILE COPY

Interhemispheric Comparison of Atmospheric Circulation Features as Evaluated from NIMBUS Satellite Data



Semi-Annual Report

1 July 1972 - 31 December 1972

Grant NGR 06-002-098

**DEPARTMENT OF ATMOSPHERIC SCIENCE
COLORADO STATE UNIVERSITY
FORT COLLINS, COLORADO**

SEMI-ANNUAL REPORT

for

Grant NGR 06-002-098

1 July 1972 - 31 December 1972

Prepared by

E. R. Reiter, Principal Investigator

Department of Atmospheric Science

Colorado State University

for

National Aeronautics and Space Administration

Contracting Officer: Mrs. G. Wiseman

Technical Monitor: Dr. V. Salomonson

General Circulation Parameters in the Troposphere and Stratosphere
as Calculated from SIRS-derived Thermal and Mass Structure

by

R. F. Adler

Department of Atmospheric Science
Colorado State University
Fort Collins, Colorado

April 27, 1973

Abstract

General circulation parameters in the northern hemisphere are calculated using atmospheric thermal structure obtained from Nimbus III SIRS multi-channel radiance information. The thermal structure up to 10 mb is obtained by using a regression technique with thickness between pressure levels as the dependent variable. General circulation parameters calculated on a daily basis include zonal and eddy available potential energy, and zonal and eddy kinetic energy. A second set of calculations is performed using National Meteorological Center (NMC) grid data. A comparison of the two sets of calculations indicates that, although the energies calculated from the SIRS-derived structure underestimate the actual energies, maxima, minima, and trends are well identified. An example of mid-stratospheric energy changes during a breakdown of the polar-night vortex is also given.

1. Introduction

The advent of satellite multi-channel radiance information, such as from the SIRS experiment, and the development of techniques to retrieve atmospheric structure from the radiances, present possibilities not only for operational uses, but for research into the global general circulation. While the general circulation of the northern hemisphere has been the subject of many studies, the general circulation of the troposphere and stratosphere of the southern hemisphere has been relatively unstudied because of the lack of a dense hemispheric radiosonde network. The ability to obtain atmospheric structure on a hemispheric basis from the satellite data opens up the possibility of making general circulation calculations in the southern hemisphere. Before making these calculations in the southern hemisphere, calculations in the northern hemisphere should be made using structure derived from both SIRS data and conventional data. The comparison of the two sets of computations will indicate the limitations of the calculations based on the satellite information. The purpose of this paper is to show examples of comparisons between calculations made from both sources of data and to show an example of energetics calculations during a stratospheric polar vortex breakdown based on SIRS-derived structure.

2. Techniques Used to Obtain Structure from SIRS Data

Atmospheric thermal structure is obtained from the NIMBUS III SIRS radiances using a regression technique similar to that of Smith, Woolf and Jacob [3] . . . However, instead of using the temperature of particular pressure levels as the dependent variable, the thickness between pressure surfaces is used. The height difference between pressure surfaces is, of course, proportional to the layer-mean temperature. For the regression analysis, the data is divided into three latitude bands: 20° - 40° N, 40° - 60° N, and 60° - 80° N. Eight layers in the vertical are used from 10 mb to 1000 mb. Cloud-contaminated data is eliminated by checking the radiances in channel 2 (750 cm^{-1}) and channel 3 (714 cm^{-1}) against pre-determined limits which are a function of latitude. If the observed radiances in both channels fall below the limits, the data is eliminated as cloud-contaminated. The radiance limits are selected by comparing observed SIRS radiances and satellite cloud photographs.

The regression equations are obtained using a near-simultaneous matchup of SIRS radiances and thicknesses obtained from the NMC northern hemisphere fields for the layers below 100 mb, and from station data for the layers above 100 mb. The root mean square errors of the regression equations are comparable to those of Smith, Woolf and Jacob [3] with errors of from 2 - 4° K. Geopotential height data is obtained by adding the thicknesses derived from the SIRS data to an NMC hemispheric 1000 mb height field.

3. Comparison of General Circulation Parameters

General circulation parameters calculated include the zonal and eddy available potential energy (AZ and AE, respectively) and the zonal and eddy kinetic energy (KZ and KE, respectively). The calculations are made on a daily basis for the month of January, 1970, and are done using a 5° by 5° latitude-longitude grid between 20°N and 80°N . The NMC data is linearly interpolated from the NMC grid to the latitude-longitude grid. The SIRS-based data is also linearly interpolated from satellite track positions to the latitude-longitude grid. Satellite data is combined for 24 hour periods centered on 1200Z to obtain substantial hemispheric coverage.

The formulations used in the calculations are as follows:

$$AZ = \sum_{i=1}^8 \frac{[(T_i)_\lambda]_{\lambda,\phi}^2}{2[\sigma]_{\lambda,\phi}} \Delta p_i \quad (1)$$

$$AE = \sum_{i=1}^8 \frac{[(T_i)_\lambda]_{\lambda,\phi}^2}{2[\sigma]_{\lambda,\phi}} \Delta p_i \quad (2)$$

$$KZ = \sum_{i=1}^8 \frac{[(u_i)_\lambda]^2 + [(v_i)_\lambda]^2}{2g} \Delta p_i \quad (3)$$

$$KE = \sum_{i=1}^8 \frac{[(u_i)_\lambda]^2 + [(v_i)_\lambda]^2}{2g} \Delta p_i \quad (4)$$

The notation follows that of Reiter [2] with brackets representing an average over the subscripted variable and parentheses representing a deviation from the average. The summation is over the eight layers in the vertical. The variable T_i represents the mean layer temperature in the i^{th} layer derived from the thickness, λ is longitude, ϕ is latitude,

u_i and v_i are the usual scalar horizontal wind speeds, Δp_i is the pressure difference from the bottom to the top of the i^{th} layer and $[\sigma]$ is the hemispheric averaged static stability given by

$$[\sigma]_{\lambda, \phi} = - \frac{g}{1000^k R} p^{1+k} \left[\frac{\partial \theta}{\partial p} \right]_{\lambda, \phi}, \quad (5)$$

where θ is the potential temperature, g is the acceleration of gravity and R is the universal gas constant. The u_i and v_i in equations 3 and 4 are calculated using the geostrophic assumption. In this paper contributions to the total energy from individual layers will be noted by, for example, AE (300-500 mb), the contribution to the total AE from the layer 300-500 mb.

In the figures to be presented, three-day running means are used to smooth out small time scale fluctuations. In addition to the smoothing of the three-day running means, seven days are eliminated from the SIRS representation because of insufficient hemispheric data coverage. The elimination is based on the number of locations in the five-by-five latitude-longitude grid that are originally filled with satellite data. The days eliminated are January 1, 5, 13, 21, 26, 28, 31.

Figure 1 shows the AZ (300-500 mb) computed from both the NMC fields and from the fields derived from the SIRS radiances. The AZ (300-500 mb) based on the SIRS data is consistently less than the NMC-based results. The underestimation is about 20%. Since AZ involves squares of terms involving meridional temperature gradients, the underestimation of AZ by 20% implies an underestimation of meridional temperature gradients by about 10%. The underestimation appears to be larger in the middle of the month. The dates of relative maxima and minima are, however, well

defined. The times of the month when there is a significant increase or decrease of AZ are indicated correctly.

Figure 2 indicates the variation of KE (300 mb) during the month as calculated from NMC 300 mb height field and the 300 mb height field obtained from SIRS-derived thicknesses added to the NMC 1000 mb height field. The KE (300 mb) actually represents the contribution to the total KE from the layer 250-400 mb. The SIRS KE underestimates the actual by about 50%. However, positions of relative maxima and minima are again indicated. Starting from a minimum at the beginning of the month, there is a sharp increase from about the 5th to a peak on the 9th, indicated in both curves. After a decrease to the 12th, the two curves do not parallel each other well until the sharp rise from the 17th to the peak around the 20th and 21st. From this peak to the end of the month, there is a sharp decrease to the low for the month in both curves.

Figure 3 gives the two curves for AE (100-200 mb). This layer is, for the most part, in the lowest part of the stratosphere. The underestimation is present again, with the SIRS AE being about 55% of the NMC values on the average. Again, however, the maxima, minima and trends are well indicated by the SIRS-based AE. The sharp increase from the 5th to the 10th is indicated well, as is the increase from the middle of the month to the maximum for the month on the 22nd. From this peak to the end of the month, there is a sharp decrease in both curves.

Figures 1 through 3 are representative examples of general circulation calculations in the upper troposphere and stratosphere. The calculations indicate that although magnitudes are systematically underestimated, especially in the eddy terms, the calculations based on SIRS-derived atmospheric structure correctly identify times of maxima, minima and major changes in components of the atmosphere's energy cycle.

4. Energy Changes during a Stratospheric Breakdown

Figure 4 shows three day running means of mid-stratosphere energy parameters during a polar vortex breakdown. The parameters have been calculated solely from thermal structure obtained from SIRS radiances, with the exception of the use of daily 1000 mb height fields. The AZ and AE in Figure 4 are the contributions to the total values from the layer 10-30 mb. The KZ and KE in the diagram are based on the 10 mb height fields and represent the layer 0-20 mb. The dashed portions of the curves indicated dates when the data is such that the indicated computations are unreliable, or days when there are missing data.

The breakdown begins about December 22. Prior to that there is a significant increase in KZ (10 mb) and KE (10 mb) from the 15th to the 19th. From the 22nd to the 28th, there is a sharp increase in AE, a sharp decrease in KZ, and a decrease in AZ. The decrease in AZ is small in magnitude but large in percentage change. The KE reaches a peak on the 27th. The AE remains high until about January 1, decreases sharply from the 1st to the 5th, and remains nearly constant for the remainder of the period. While the AE decreases, the AZ increases to a peak on the 3rd and 4th and then decreases again. After reaching its peak on the 27th, the KE decreases unsteadily.

One interesting observation from Figure 4 is that the sum of the four energies decreases from before to after the stratospheric breakdown. Because it is unlikely that generation or dissipation terms could account for this decrease, the decrease implies an export of energy out of this mid-stratospheric layer during the breakdown.

The breakdown in Figure 4 has been studied by Miller, Brown and Campana [1] using mainly NMC and rocketsonde data. The energy changes

in Figure 4 agree at least qualitatively with their calculations.

Quantitatively, it is difficult to compare the computations since different layers and different geographic areas are used in the computations.

5. Conclusions

The examples shown in this paper indicate that, within the limitations discussed, worthwhile general circulation calculations can be made with atmospheric structure derived from satellite, multi-channel radiance data.

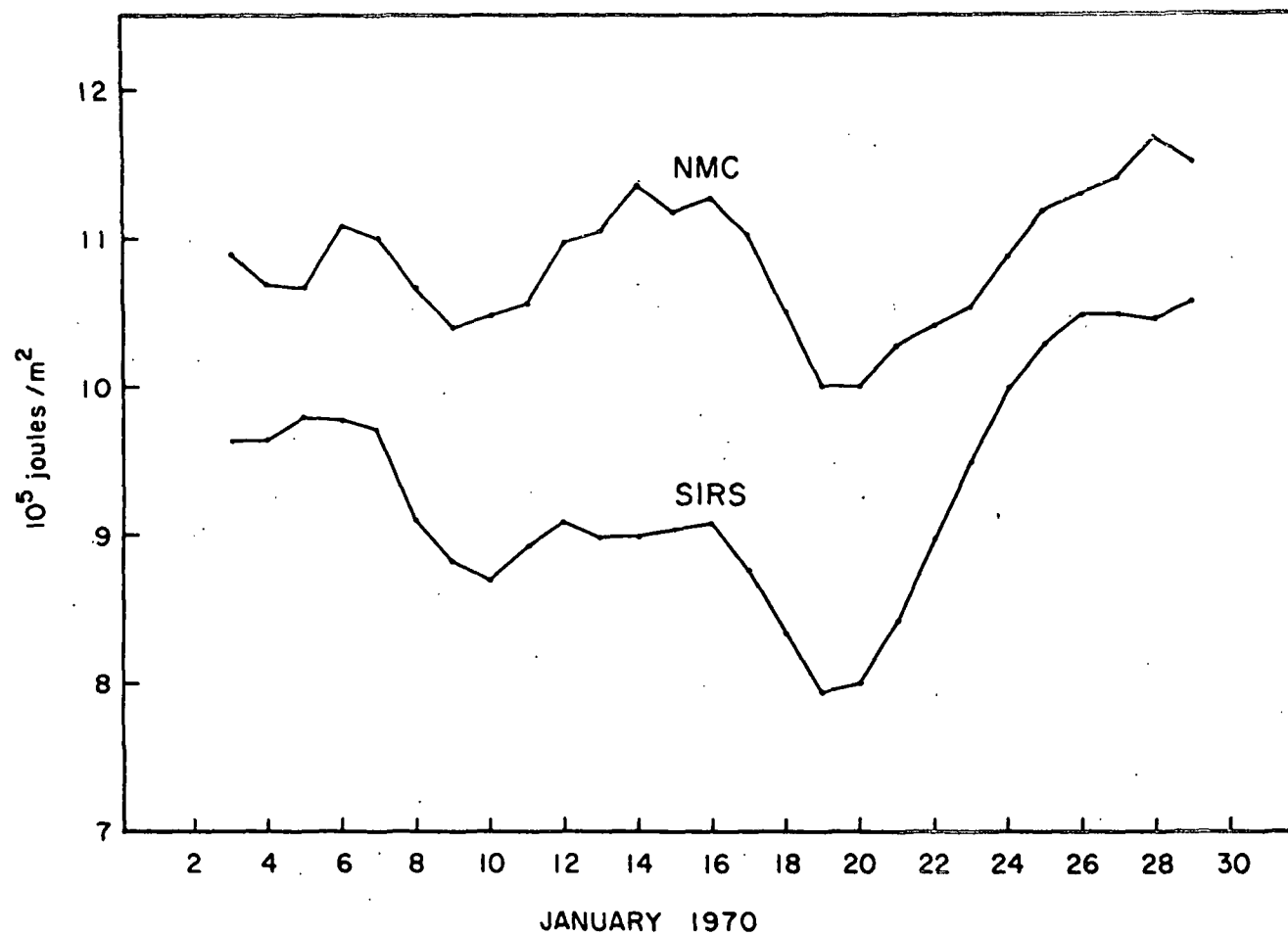


Fig. 1. Variation with time of the contribution to the zonal available potential energy from the 300-500 mb layer, AZ [300-500 mb].

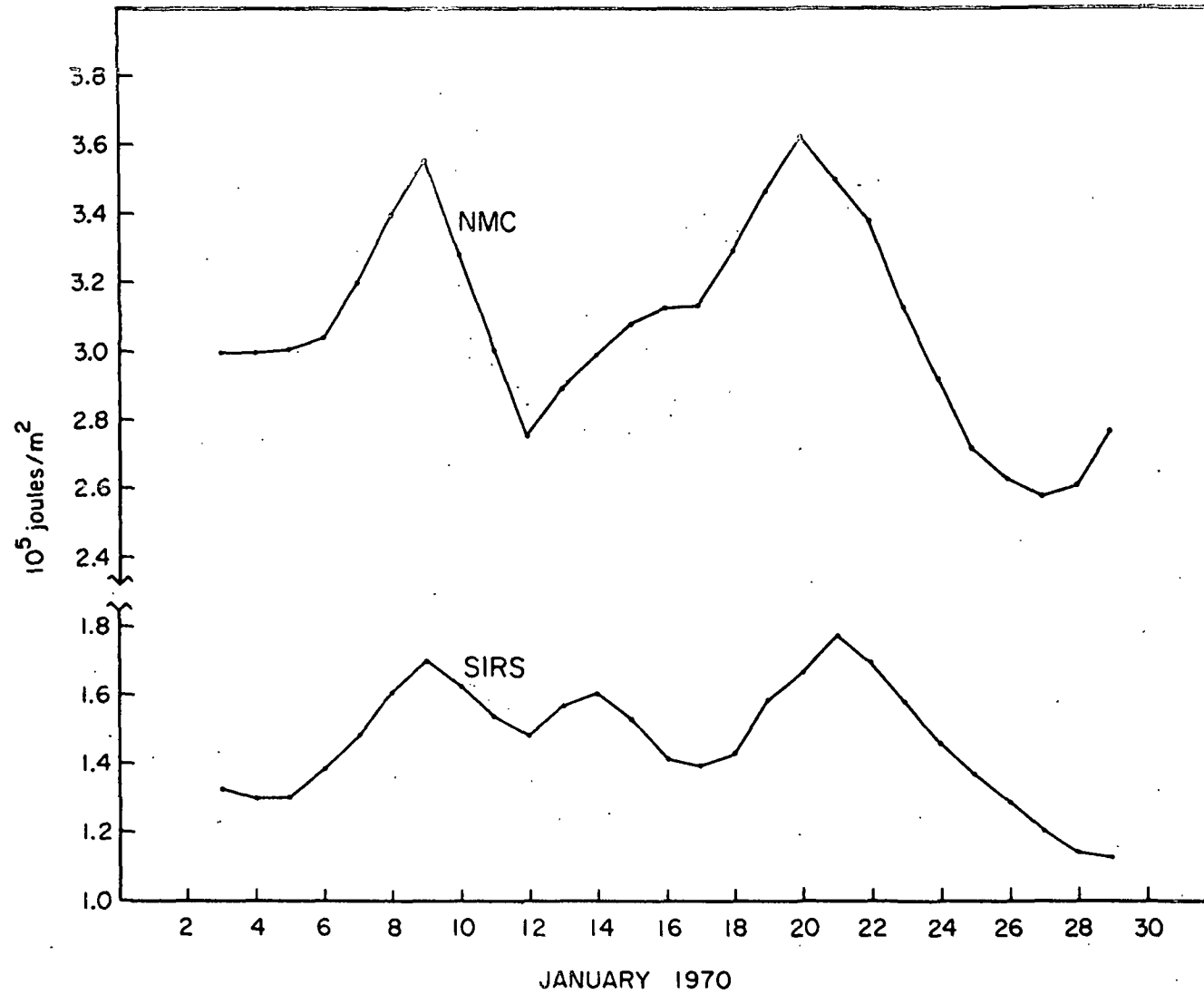


Fig. 2. Variation with time of the eddy kinetic energy at 300 mb, KE [300 mb].

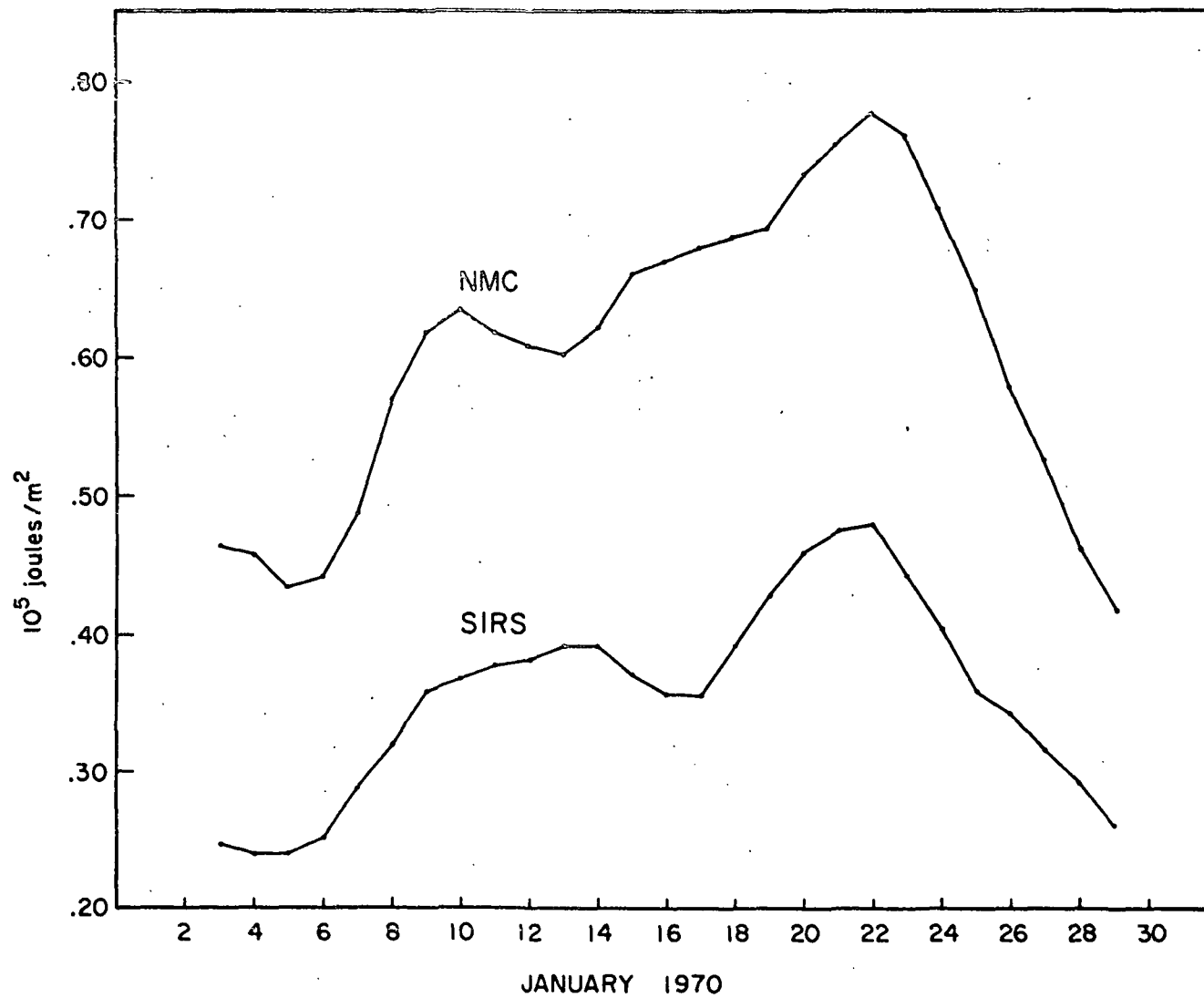


Fig. 3. Variation with time of the contribution to the eddy available potential energy from the 100-200 mb layer, AE [100-200 mb].

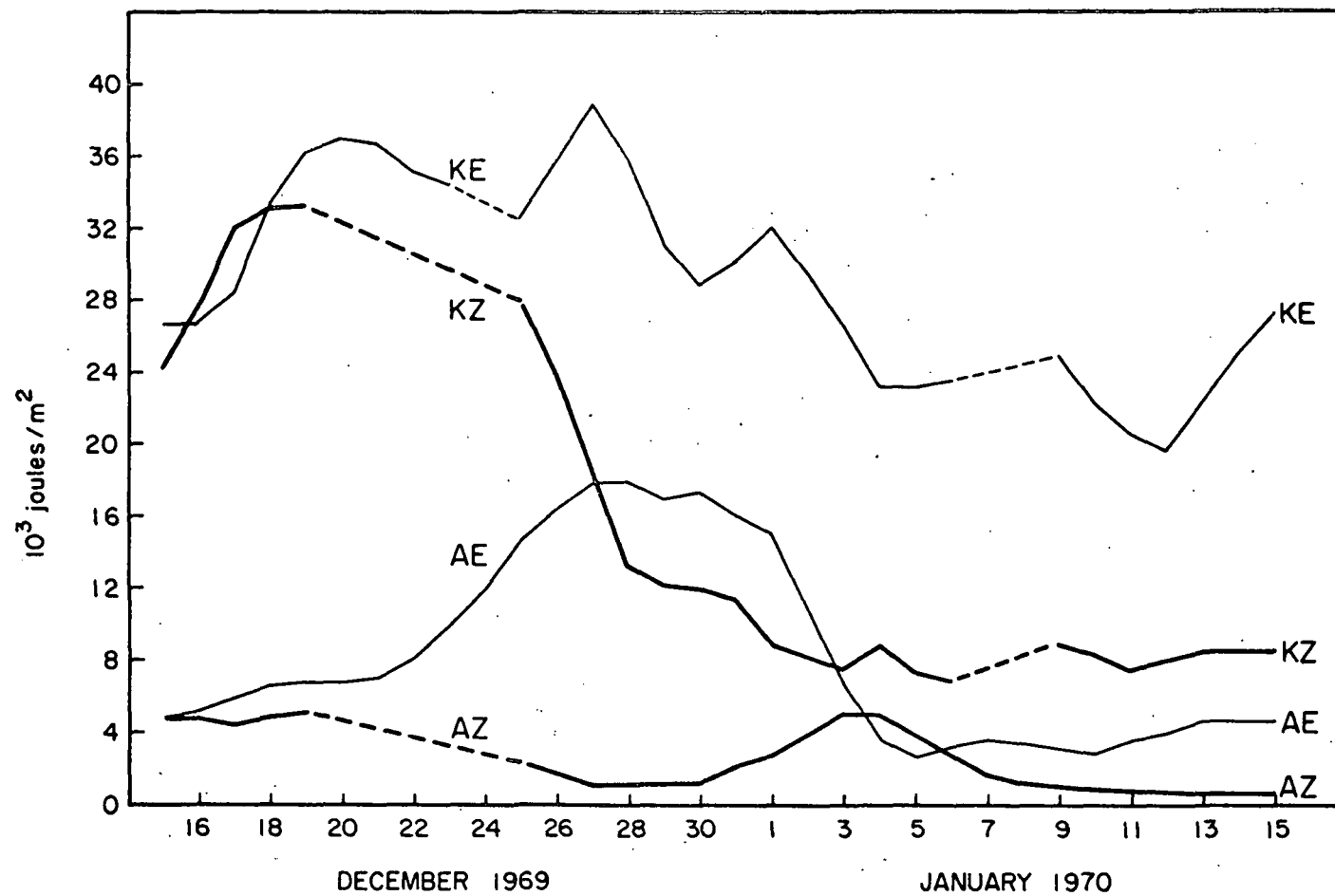


Fig. 4. Energy changes during a stratospheric breakdown. AZ and AE for the 10-30 mb layer, KZ and KE at 10 mb.

References

1. Miller, A. J., J. A. Brown and K. A. Campana: A Study of the Energetics of an Upper Stratospheric Warming (1969-1970). Quart. J. Roy. Meteor. Soc., 98, 730-744 (1972).
2. Reiter, E. R.: Atmospheric Transport Processes, Part I: Energy Transfers and Transformations. AEC Critical Review Series, USAEC Report TID-24868. Oak Ridge, Tennessee: USAEC Division of Technical Information Extension, 1971.
3. Smith, W. L., H. M. Woolf and W. J. Jacob: A Regression Method for Obtaining Real-Time Temperature and Geopotential Height Profiles from Satellite Spectrometer Measurements and Its Application to Nimbus 3 SIRS Observations. Monthly Weather Review, 98, 582-603 (1970).